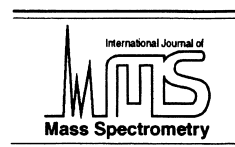




ELSEVIER

International Journal of Mass Spectrometry 205 (2001) 171–182



Spectroscopy and dynamics of nitromethane (CH_3NO_2) and its anionic states

Isobel C. Walker^{1,*}, Malcolm A.D. Fluendy²

¹Department of Chemistry, Heriot-Watt University, Riccarton, Edinburgh EH14 4AS, Scotland, UK

²Department of Chemistry, University of Edinburgh, West Mains Road, Edinburgh EH9 3JJ, Scotland, UK

Received 5 June 2000; accepted 16 July 2000

Abstract

Dissociative electron attachment in nitromethane has been investigated along with related spectroscopic measurements made using optical and electron scattering methods. The nature and dissociation dynamics of the low-lying anionic states of nitromethane are discussed in the light of these experiments and the results of ab initio molecular orbital computations. (Int J Mass Spectrom 205 (2001) 171–182) © 2001 Elsevier Science B.V.

Keywords: Dissociative electron attachment; Anionic states; EELS; VUV

1. Introduction

Nitromethane (CH_3NO_2) is the simplest organic–nitro compound and so is an important prototype molecule. For example, as is typical of this class of compound, it is an explosive; elucidation of the complex processes involved in its detonation and propellant behaviour requires understanding of the electronic states of both neutral and ionic species. Also, it may play a role in atmospheric chemistry following reaction of methyl (CH_3) radicals with oxides of nitrogen. In this article, we present the results of a number of spectroscopic studies on nitromethane, directed mainly at the elucidation of its anionic states. These have been implicated as gateway states in many of its reactions and interactions and

have been investigated both directly (with electron-impact techniques) and less directly (in alkali atom or Rydberg atom scattering). However, uncertainties and ambiguities exist both in the experimental data and their interpretation and these systems remain of interest as relatively simple examples in which competing dynamics involving both nuclear and electronic motion can be studied.

1.1. Spectroscopy and dynamics: neutral CH_3NO_2

The frontier molecular orbitals (MOs) of nitromethane are shown schematically in Fig. 1; these pictures were obtained from the results of an ab initio computation described later. As illustrated, for the three highest occupied orbitals and the lowest unoccupied one, electron density is concentrated at the NO_2 end of the molecule. Consequently, the spectroscopy of nitromethane is usually discussed in C_{2v}

* Corresponding author. E-mail: i.c.walker@hw.ac.uk

Dedicated to Professor Aleksandar Stamatovic on the occasion of his 60th birthday.

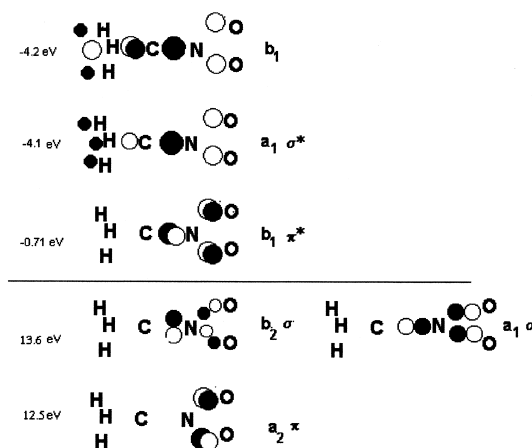


Fig. 1. Schematic of orbitals in nitromethane. The labeling is based on C_{2v} symmetry and the drawn size (open and closed circles) is a guide to the relative contribution of the components in each orbital. The atoms, H, C, N, and O are in bold characters.

symmetry although, strictly, the molecule belongs to the C_s point group (and transitions involving the CH_3 group might be described in C_{3v}). The three highest occupied MOs are of (C_{2v}) symmetry $a_1(\sigma)$, $a_2(\pi)$, and $b_2(\sigma)$, the last frequently described as n , nonbonding.

In the He(I) photoelectron spectrum of nitromethane each of the first two bands, adiabatic ionisation energies 11.07 and 11.32 eV, respectively, shows a vibrational progression, spacing about 0.070 eV, ascribed to excitation of the ONO bending mode (0.081 eV, 657 cm^{-1} in the neutral ground state). Bands 3 and 4 are broad and structureless [1,2]. From the appearance of the spectrum, Rabelais [1] assigned bands 1–3 to cationic states 2A_1 , 2B_2 , and 2A_2 in that order. Others [3] have claimed that photoelectron angular distribution measurements (unpublished) show the above three states to be involved in the first two bands with two ionisations in band 2. This possibility was proposed by Murrell et al. [4], following a theoretical treatment in which ionisation from the two σ orbitals, (2A_1 , 2B_2) could not be separated. Most computations (including the present) find the highest occupied orbital (HOMO) to be $a_2(\pi)$ [4–6] with the $b_2(\sigma)$ and $a_1(\sigma)$ orbitals almost degenerate.

There has been little progress in our knowledge of

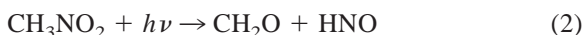
the electronic spectrum over that summarised by Flicker et al. in 1972 [7]. All reported optical bands are broad and structureless. The most intense of these, centred around 6.25 eV, is ascribed to excitation of a state of type $\pi\pi^*$ (1B_2 , $a_2b_1^*$). A weak absorption around 4.5 eV has been assigned to excitation of state ${}^1\sigma\pi^*$ (1B_1 , $a_1b_1^*$) [5,6,8]. Flicker et al. [7], from angular distribution measurements on inelastically scattered electrons, suggested that a second spin-allowed transition lies close to the 1B_1 state in energy. Angular distribution data also led to location of a triplet excited state, $E_{\text{max}} = 3.8\text{ eV}$, assigned ${}^3\pi\pi^*$ (3B_2).

Photodissociation following excitation within the 6.25 eV ($\pi\pi^*$) band has been studied extensively, most recently with pulsed laser techniques [9–12]. Dissociation is rapid and appears to involve rupture of only the C–N bond



In a simple MO picture both the lower (π) and upper (π^*) orbitals are concentrated on the NO_2 moiety, so that in the final excited state a repulsive interaction along the C–N coordinate is unlikely. Both electronic and vibrational predissociations have been suggested, the former (and dominant) by a state of type $\sigma\sigma^*$ (1B_2 , $b_2a_1^*$) leading to NO_2^* [2B_2 , which further dissociates to NO (X) and O] and the latter, through coupling between NO_2 and CN vibrations on the $\pi\pi^*$ (1B_2) surface, producing NO_2^{**} (2B_2) [9,11,12]. Reaction (1) also appears to be a primary dissociation pathway within the 4.5 eV band but data relating to this spectral region are confused. NO_2 has been observed following irradiation at 252.6 nm (4.91 eV) [13] and 264 nm (4.7 eV) [14]. Kwok et al. [15] failed to detect any dissociation products after collision-free absorption at 266 nm (4.66 eV) while others claim that NO_2 is formed within 5 ps of absorption of a 266 nm photon [16]. The hydroxyl radical, OH, was reported as a primary product many years ago [17]. A recent measurement gave a quantum yield of 0.004 at 266 nm [18]; however, OH was not detected at 282 nm (4.4 eV) [19]. Early workers [20] proposed that photoabsorption at 313 nm (3.96 eV) leads to reaction

(1) and, from experiments carried out in the presence of different gases, ascribed it to dissociation of the lowest triplet state whose energy they estimated to lie above the onset energy of the triplet state in ethene; this would place it above about 3.5 eV. Further, they deduced that the lowest singlet excited state dissociates by means of



1.2. Spectroscopy and dynamics: negative ions

CH_3NO_2^-

Nitromethane has a positive adiabatic electron affinity. Photoelectron measurements led to a value of 0.26 ± 0.08 eV [21] which is close to the theoretical result (0.22 eV) computed by Gutsev and Bartlett [22]. However, these values are at odds with that determined by using electron capture data, recently reported as 0.5 ± 0.02 eV [23] and it has been suggested that the lower estimate (0.26 eV) relates to an excited state of the anion [23]. In any event, the ground anionic state is of 2B_1 symmetry, having the extra electron in the π^* (b_1) orbital. All calculations on this species find it to have tetrahedral geometry at N and an elongated N–O bond [22,24].

The parent negative ion is not observed in the gas phase following impact with a free electron under single collision conditions, but has been collected in high pressure electron-swarm systems [25]. It is also formed when the incoming slow electron is either in a highly excited atomic Rydberg state [21,25] or bound to an alkali atom [26–28]. For these processes the vertical electron affinity (EA_v) is a relevant quantity. EA_v is reported by Gutsev and Bartlett [22] as being negative at all levels of theory, while the present calculations (below) yield a vertical affinity of -0.7 eV (cf. -0.2 eV adiabatic). The dipole moment of nitromethane (3.46 D) is well above the lower limit for formation of a dipole-bound anion and, under appropriate conditions, a Rydberg electron can transfer to make the dipole-bound anion [21]. Further, it seems likely that the dipole-bound and conventional

valence anion are coupled so that one can act as a gateway to the other [21,22].

Excited anionic states have been probed mostly through dissociative electron attachment (DEA) processes such as



This kind of channel is available only if the vertical electron affinity is negative. It has been established that NO_2^- is produced [probably by means of reaction (3)] on impact of nitromethane with electrons of energy around 0.6 eV [25,29,30]. At higher incident-electron energies, the major ionic product is O^- , but reported attachment energies vary [25,29,30]. In addition, almost all possible fragments having positive electron affinities and which can be assembled from the constituent atoms have been detected [25,29,30]. However, care must be taken in relating these to cross sections for primary processes since the rates of possible ion–molecule reactions are large [30]. As will emerge later, the present DEA results resemble most closely those of Di Dominico and Franklin [30].

Additional information on the anionic states of nitromethane has come from the analysis of the behaviour of the neutral molecule on impact with ground-state alkali atoms. Sholeen and Herm [31] explored reactive scattering of Li with CH_3NO_2 to give LiNO_2 and CH_3 and concluded that reaction proceeds through a 2A_1 (σ^*) anion formed either directly or by means of internal conversion from a 2B_1 (π^*) precursor. The ($\text{K} + \text{CH}_3\text{NO}_2$) system has been studied in both ionic and inelastic channels. In the former, CH_3NO_2^- , NO_2^- , and O^- were detected along with K^+ [28]. Three anionic states, namely a repulsive, σ^* state (2A_1) and two bound 2B_1 (π^*) states were invoked as intermediates in the ion production. A vertical electron affinity of -2.16 ± 0.7 eV was deduced for the excited 2A_1 (σ^*) state and it was observed that the 2A_1 anion decays by means of autodetachment



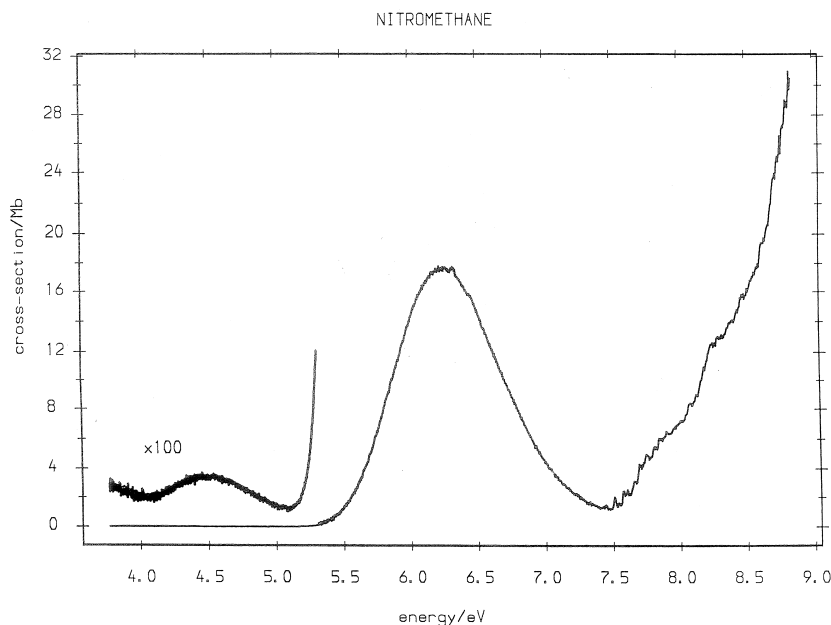


Fig. 2. VUV spectrum of nitromethane.

as well as dissociation [28]. These results supported conclusions from earlier measurements on potassium and sodium atoms inelastically scattered from nitromethane [32]. In these, several energy-losses were observed and ascribed to sequential electron transfer from atom to molecule and back again by way of intermediate anionic states which included a dissociative σ^* resonance and at least one π^* anion.

Emission and absorption spectra observed in a shock tube experiment were ascribed to transitions between anionic states ($\Delta E = 2.2$ eV); if this is the case, then anionic mechanisms are important in the detonation of molecules containing the nitro group [33].

We have now (1) re-measured and extended the photoabsorption spectrum by using a synchrotron radiation source (2) obtained near-threshold electron energy-loss (EEL) spectra in a search for optically forbidden electronically excited states and autodetaching anionic states and (3) recorded DEA spectra with both mass and energy analysis of the product ions. These experimental results are reconciled with each other and with previously reported data with the aid of MO computations.

2. Methods

2.1. Photoabsorption apparatus

Optical spectra were recorded at the CLRC Synchrotron Source, Daresbury, using the Daresbury Laboratory Molecular Sciences Absorption Apparatus (DLMSAA) coupled to beam line 3.1. The apparatus has been described in [34]. Briefly, the synchrotron light enters and leaves the absorption cell through LiF windows. The transmitted radiation is detected by using a sodium salicylate quantum converter and photomultiplier tube. The absorption path length within the cell is 16 cm. Experiments were carried out with static gas samples. Thus radiation transmitted through the sample, I_t , was recorded at each wavelength as was the sample pressure (measured on a Baratron capacitance manometer) and the decreasing synchrotron ring current. The radiation transmitted through the empty cell, I_0 , was then monitored along with the ring current at the same selected wavelengths. Digitised data were stored on a computer. The transmitted radiation was normalised to a constant ring current before data analysis using the

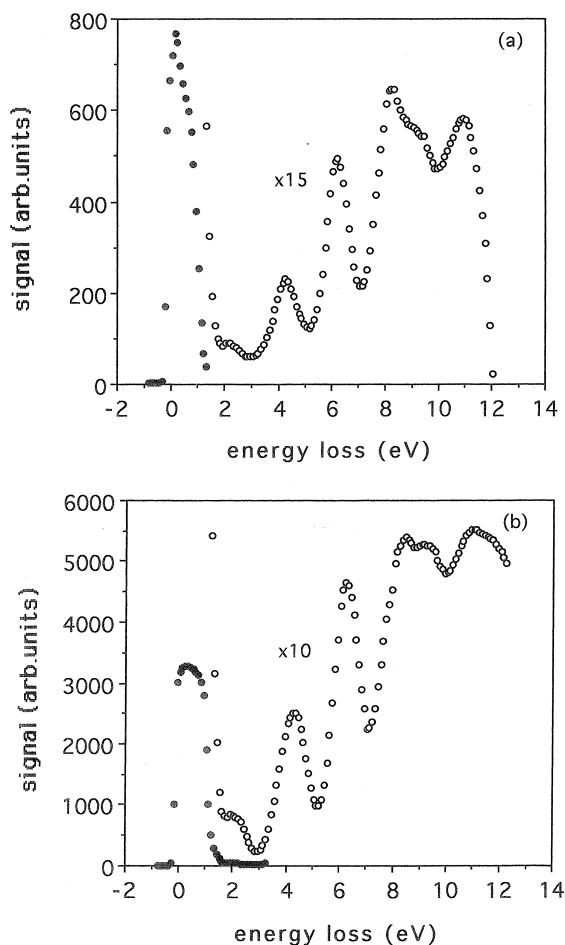


Fig. 3. EEL spectra of nitromethane, at residual electron energy, E_r : (a) ≈ 0.2 eV and (b) ≈ 0.5 eV.

Beer-Lambert expression: $I_t = I_0 \exp(-\sigma_{pa} N x)$, where N is the target number density, σ_{pa} the photoabsorption cross section, and x the path length.

2.2. Electron impact apparatus

Electron impact data were obtained using two different spectrometers. The first, a trapped electron spectrometer, has been described [35]. Briefly, in this, a monochromatic beam of electrons (selected in a trochoidal electron monochromator and so moving under the influence of an axial magnetic field) is transmitted through the target gas as the electron energy is stepped from zero upwards. The electrode

potentials in the collision region are such that any inelastically scattered electrons whose energy is between 0 and a pre-set value eW are trapped in a potential well and collected. The resulting spectrum is a near-threshold electron energy-loss spectrum at a residual electron energy of eW . In this mode, the energy-loss axis was calibrated from the helium transition at 19.81 eV (2^3S). As well as low energy electrons, negative ions formed in resonant dissociative electron attachment are collected; these can be identified because they persist at zero well depth, when electrons are no longer trapped. For these, the incident electron energy was calibrated with reference to the peak for Cl^-/CCl_4 [36] at 0 eV electron energy.

The second system, a negative ion mass spectrometer, was employed for further analysis of negative ions detected in the electron trap system. As has been described [37] this enables both mass and energy analyses of ions formed in the collision region. The apparatus has cylindrical symmetry. An end plate to the collision region contains a cut-out annulus, width 1 mm and radius 10 mm; ions which diffuse to the annulus are extracted and focused to the entrance of a cylindrical mirror analyser for energy analysis. The energy-selected ions are then transferred to a quadrupole mass spectrometer (QMA, Vacuum Generators SXP 300) for mass analysis. Energies were calibrated with reference to an O^- signal from DEA to O_2 (O^-/O_2) [38] and F^-/SF_6 [39]. This spectrometer functions only for incident electron energies in excess of about 3 eV. All ions reported showed an extended linear range of variation with CH_3NO_2 pressure thus confirming that the tabulated ions are produced in primary processes

2.3. MO computations

A limited range of computations based on the GAUSSIAN 94 methodology [40] were undertaken in order to relate the observed spectroscopy and dynamics of the CH_3NO_2 negative ion (in particular) to a molecular orbital picture. The well known difficulties associated with the computation of negative ion states, and, a fortiori, excited ion states, means that high accuracy cannot be expected. A descriptive level

Table 1
Electronic states of nitromethane

Energy (eV)								
Experiment				Theory			Assignment	
VUV	EEL		Molecular beam					
Present	Present	[43]	[7]	[32]	[5]	[6]	[8]	
			3.8	3.5	3.01	3.13		${}^3B_2(\pi\pi^*)$
					3.71			${}^3B_1(\sigma\pi^*)$
					4.60			${}^3A_2(\sigma\pi^*)$
	4.25	4.3		4.3	4.56	3.86	4.22	${}^1A_2(\sigma\pi^*)$
4.5			4.45		4.41	3.41	4.58	${}^1B_1(\sigma\pi^*)$
6.25	6.23	6.1	6.23	6.5	5.8	6.43	6.63	${}^1B_2(\pi\pi^*)$
7.44								${}^1A_2(\pi3s^*)$
7.8		7.8		7.6				valence
8.07								$\sigma3s$
8.3	8.3	8.2	8.3	8.5				valence
			8.85					
	9.1	9.3	9.43	8.8–9.2				

of detail is nevertheless of considerable value in determining orbital character and ordering. The basis set 6-311++G(2d,2p) was used throughout this study. This basis was found, in the more extensive investigation of Gutsev and Bartlett [22], to give a good account of the negative ion energetics, a more taxing task than calculation of the geometry. Ground state neutral and negative ion computations were made at the second-order Møller-Plesset level; the excited states were investigated at the configuration interaction singles level. The orbital picture arising from these computations is shown in Fig. 1.

3. Results

3.1. Neutral CH_3NO_2

The optical spectrum (Fig. 2) agrees with the literature, both in excitation energy and cross section over the two low-energy bands whose E_{\max} values are 6.25 eV (${}^1B_2, \pi\pi^*$) and 4.5 eV (${}^1B_1, \sigma\pi^*$), respectively [41,42]. The assignments are in accord with theoretical predictions [5,6,8]

EEL spectra (Fig. 3) also show the 6.25 eV transition. However, the cross section in the lower band has its maximum value at 4.25 eV rather than the

optical value of 4.5 eV. The angular measurements of Flicker et al. [7] suggested the presence of a weak spin-allowed transition in this energy region. The combined EEL data, taken together with the results of computations, lead to the assignment of the 4.25 eV feature to excitation of the ${}^1A_2(\sigma\pi^*)$ state; this is symmetry forbidden in the C_{2v} point group and hence not obvious in the optical absorption spectrum. The triplet states, 3B_1 and 3A_2 are expected to be close by. Interestingly, the cross section for excitation of the 3.8 eV triplet state (${}^3B_2, {}^3\pi\pi^*$), reported by Flicker et al. [7], is negligible at near-threshold electron energies. The main features of the present EEL spectra are seen also in the data of McAlister [43] who used an electron-scavenger technique (Table 1).

No Rydberg-excited states have been reported for nitromethane. We now link the weak fine structure, onsetting at 7.44 eV in the optical spectrum (Fig. 2) to the excitation of such a state. The vibrational structure is irregular, but we can extract a progression, spacing around 0.06 eV, which is close to that in the first two bands of the photoelectron spectrum. From the Rydberg expression, $E_{\text{ex}} = -R/(n - \delta)^2$ and with $E_{\text{ex}} = 7.44$ eV, $R = 13.6$ eV, and $\text{IE} = 11.07$ eV, the quantum defect δ is 1.06; this denotes excitation of an electron from the highest occupied molecular orbital

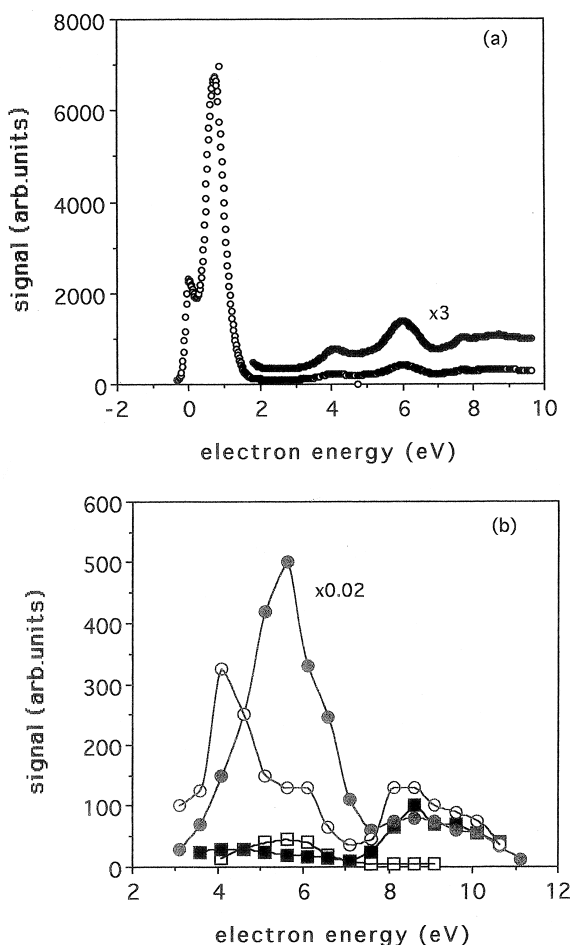


Fig. 4. Negative ions from nitromethane (a) Total negative ion signal; the peak at 0 eV is the energy marker (Cl^-/Cl_2). (b) Individual ion intensity vs. electron energy (all near-thermal ions): O^- (closed circle); OH^- (open circle); CH^- (open square); CN^- (closed square). (CNO^- was also detected with an ion yield curve which resembles that of CN^-); symbols are data points which have been joined to aid the eye.

to a $3s$ Rydberg orbital. The very low intensity of the absorption is consistent with excitation of a state which is electric-dipole forbidden in the C_{2v} point group, namely 1A_2 , and so supports the assignment of the HOMO as a_2 (π) [4–6]. We also tentatively assign weak structure starting at 8.07 eV to excitation of a second $3s$ Rydberg state linked to IE_2 (11.69 eV, $\delta = 1.06$). A shoulder around 7.8 eV is taken as excitation of a valence state. Another shoulder in the optical spectrum around 8.3 eV is strong in our EEL

spectra, but more guidance is required before assignment of this and higher bands (Table 1).

The energy-loss peak just above 2 eV in the EEL spectra (Fig. 3), recorded with residual electron energies in excess of about 0.1 eV, is assigned to resonant vibrational excitation of the ground state molecule by way of an autodetaching resonance. From spectra recorded at different residual electron energies, we position the resonance energy at about 2.4 eV. There are additional energy losses around 1 eV that we also ascribe to resonant vibrational excitation. These are discussed further in the following.

Excitation energies and proposed assignments are tabulated in Table 1. This table contains, also, energies evaluated from the inelastic scattering of K and Na atoms from nitromethane [32] and which are in agreement with the spectroscopic measurements.

3.2. CH_3NO_2^-

The total negative ion signal [Fig. 4(a)] shows maxima at incident electron energies of 0.72, ≈ 4 , ≈ 6 , and 8–9 eV. These resonance energies match those reported by Di Domenico and Franklin [30], except for the 6 eV maximum which is displaced in energy from their value of 5.6 eV; however, we can account for this (see the following). No negative ions are detected around 2 eV where others have reported production of CN^- [25,29] and CNO^- [29]; these 2 eV data have been used very recently [23] in the construction of potential energy curves for the anionic states of nitromethane. Given the sensitivity of the present experiment we are confident that negative ions are not produced at around 2 eV in nitromethane and therefore suppose that the ions previously recorded originated in an impurity. However (see previous discussions and Fig. 3), there is an anionic state at about this energy, which decays to the vibrationally excited neutral ground state following autodetachment.

Mass analysis of the ions identified the species listed in Table 2 [and Fig 4(b)]. As indicated previously, the spectrometer did not function below 3 eV and so we cannot confirm that NO_2^- is the exclusive product at 0.7 eV. There is good agreement between

Table 2
Major decay products following free electron attachment to $\text{CN}_3\text{NO}_2^{\text{a}}$

Energy (eV)	~2.4		0.72		~4.0		~5.6		~6.1		~8.6	
			present	[30]	present	[30]	present	[30]	present	present	[30]	
	$\text{CH}_3\text{NO}_2^{\text{vib}} + e$		NO_2^-				O^-	O^-	O^-	O^-	O^-	
					OH^-	OH^-	OH^-	OH^-		OH^-	OH^-	
					CN^-	CN^-		CN^-		CN^-	CN^-	
					CNO^-	CNO^-		CNO^-		CNO^-	CNO^-	
							CH^-	CH^-				
								NO^-				
												NO^-
												HCNO_2^-
												H_2CNO_2^-

^a Ions recorded in [30] and which, as discussed by the authors, may have been formed in ion/molecule reactions have been omitted.

the present data and those of Di Domenico and Franklin [30], when account is taken of the probable secondary ions observed by these earlier workers. The most abundant ion (apart from NO_2^- at 0.72 eV) is O^- followed by OH^- . All the ions had around thermal energy except for some O^- ions in the 6 eV resonance region. There, in addition to a thermal branch whose attachment cross-section has its maximum value at 5.6 ± 0.2 eV (in accord with the energy reported by Di Domenico and Franklin [30]), a group carrying about 1 eV of kinetic energy was detected [Fig. 5(a)]. The cross-section maximum for this group is at an incident electron energy of 6.1 ± 0.2 [Fig. 5(b)]. Taking these two channels together, the E_{max} value is close to 6.0 eV, as measured in the total ion experiment.

The results of the quantum computations for the states of the negative ion are shown in Table 3 with a qualitative indication of their composition.

4. Discussion

Our discussion centres on the anionic states of CH_3NO_2 . A significant body of data now exists relating to the negative ion in various states and its role in collision dynamics. It remains to produce a coherent picture. From the current experiments we find direct evidence for anionic states at (electron attachment energies) around 0.72, 2.4, 4, 5.6, 6.1, and

above ≈ 8 eV. Of these, all except the 2.4 eV state (which has not been detected previously in electron scattering) are seen to dissociate in these experiments. The 2.4 eV anion, as discussed in the following, decays by autodetachment to the vibrationally excited ground state of the neutral molecule.

Anions formed by capture of an electron may be based either on the neutral core configuration (one particle) or on a cationic core with two electrons in previously unoccupied orbitals (one hole, two particle). From their attachment energies, 0.72 and ~ 2.4 eV, the first two anions listed must result from accommodation of the electron in an unoccupied orbital of the ground state neutral molecule. The 4 and 6 eV anions may result from trapping by either the ground state neutral core or the valence excited states (type $\sigma\pi^*$ and $\pi\pi^*$) which lie around these energies (Fig. 2).

We assign the 0.72 eV (DEA) and ≈ 2.4 eV (resonant vibrational excitation) states as 2B_1 and 2A_1 , respectively. The former results from capture of the incoming electron in the b_1 (π^*) orbital and the latter in orbital a_1 (σ^*). In support of this, the calculated vertical electron affinity (the negative of the attachment energy) is -0.7 eV (2B_1) and -3.2 eV (2A_1), respectively. The 2B_1 state is, from the computations, the ground state of the anion; this has been detected in the alkali ion experiment of Lobo et al. [28] and following transfer of Rydberg electrons [21,27]. This

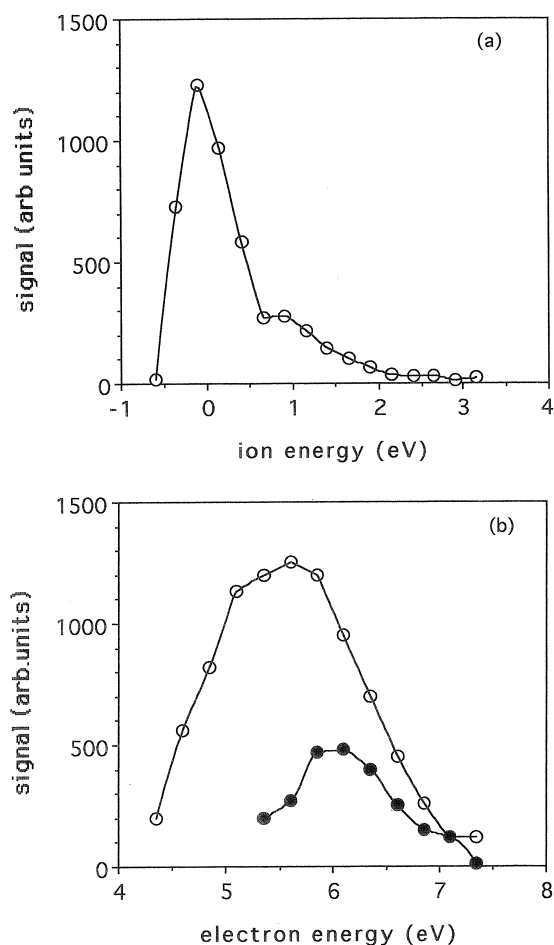


Fig. 5. O^- ions from nitromethane (a) O^- intensity vs. O^- energy at an incident electron energy ≈ 5.6 eV (b) O^- intensity vs. incident electron energy, O^- (open circle) having near-thermal energy; O^- (closed circle) having ≈ 1 eV translational kinetic energy; symbols are data points which have been joined to aid the eye.

2B_1 state of $CH_3NO_2^-$ must correlate with an excited (3B_1) state of NO_2^- , which, from experiment and theory, lies ≈ 2.7 eV above the ground 1A_1 state of NO_2^- [44]. The 2B_1 anion is therefore strongly bound along the C–N coordinate (Fig. 6). The computations on this state predict an extended NO bond and suggest that a maximum of 0.6 eV, mostly in the symmetric mode of the NO_2 group, may enter vibration. Thus, if prepared by capture of a free, low-energy electron from the neutral geometry, this state will be vibrationally excited in a C–N and N–O stretch mode. As

long as the vibrationally excited anion lies above the ground-state neutral in energy, it may decay by autodetachment; there is evidence of this in the vibrationally inelastic channel at low energy losses (Fig. 3).

The observation of a strong NO_2^- ion signal at 0.7 eV incident electron energy must follow curve crossing from the 2B_1 to a dissociative state. We suppose this to be the 2A_1 (σ^*) anion which correlates with ground state (1A_1) NO_2^- (Fig. 6). The 2B_1 anion is detected intact only in systems that enable relaxation of the initially prepared anion to vibrational levels which lie below the neutral (so precluding autodetachment) and out of reach of the crossing with the 2A_1 state. This happens in three-body collisions or in the presence of the cationic partner which results from the transfer of a bound electron.

From the previous arguments, we might expect direct capture into the dissociative 2A_1 state to produce NO_2^- ions at about 2.4 eV incident electron energy and with a translational energy of about 0.5 eV, after allowing for the kinematics. No such ions are seen. We conclude that in the free electron process the 2A_1 state autodetaches before the geometry expands sufficiently to configurations where the ion has an energy less than that of the neutral molecule and detachment ceases. The neutral molecule is thus left in an extended, vibrationally hot geometry. The alkali atom inelastic scattering measurements [32], similarly showed vibrational excitation by way of transient population of the 2A_1 state. In the ionic exit channel ($K^+ + CH_3NO_2^-$) Lobo et al. [28] also observed electrons from autodetachment and noted that product NO_2^- ion was seen only from the “covalent” scattering branch, which spends the minimum time in the 2A_1 state and so competed successfully with the auto-detachment channel. The estimated vertical electron affinity for the 2A_1 state deduced from this molecular beam work, -2.16 ± 0.7 eV, is consistent with the present value of ≈ -2.4 eV.

The identification of the anions responsible for the features seen in DEA at electron energies of 4, 5.6, and 6 eV is more difficult. As can be seen from Table 3 a number of single-particle resonances are predicted to lie in the energy range 4–5 eV; in addition, the

Table 3
Anionic states of nitromethane

-EA _v /eV		Anionic state (and nature)	Decay products		
Observed	Calculated (orbital number)		Electron impact	Alkali beam	
				[28]	[32]
0.72	0.7 (17)	2B_1 (π^* NO)	NO ⁻ (via 2A_1) CH ₃ NO ₂ ^{vib} + e	CH ₃ NO ₂ ⁻ O ⁻	CH ₃ NO ₂ ^{vib} + e
2.4	3.2 (18)	2A_1 (σ^* CN, σ^* CH)	CH ₃ NO ₂ ^{vib} + e OH ⁻ , CN ⁻ , CNO ⁻	NO ₂ ⁻ CH ₃ NO ₂ ^{vib} + e	CH ₃ NO ₂ ^{vib} + e
~4.0	4.1 (19) 4.2 (20) 4.6 (21)	2B_1 (see text) 2B_2 (σ^* CH ₃ , σ^* CH ₄ , σ^* OO) 2A_1 (σ^* CN, σ^* NO)	OH ⁻ , CN ⁻ , CNO ⁻	a CH ₃ NO ₂ ⁻ a NO ₂ ⁻ a O ⁻	CH ₃ NO ₂ ^{vib} + e
~5.6	5.5		O ⁻ , OH ⁻ , CH ⁻		
~6.1	6.0		O ⁻ ,		
~8.6	6.1		O ⁻ , OH ⁻ , CN ⁻ , CNO ⁻		

^a Assigned to an excited state of 2B_1 symmetry.

possible involvement of excited states (two-particle, one-hole resonances) must also be considered. The main feature of the 4 eV resonance region is production of OH⁻. Also, no negative ions are collected whose formation requires rupture of the C–N bond. Of the singly occupied orbitals in this energy region, orbital 19 is C–N nonbonding and orbital 20 C–N bonding in character. In each case the computed force constants (around the vertical geometry) are CN attractive. Also, the calculated electron density on the out-of-plane H atom in orbital 19 is large and is, incipiently at least, OH bonding. The computed forces around the vertical geometry in this case suggest that the molecule will distort, especially about the HCNO dihedral angle, to narrow the OH distance. Very tentatively, we ascribe initial electron capture into orbital 19 (2B_1 in C_{2v} symmetry) as the precursor to the dynamics observed at about 4.0 eV. The detailed dynamics remain unclear.

The interpretation of the processes seen at higher electron energies is more problematic. Around 6 eV, we detect two distinct dissociation channels, one to produce thermal O⁻ ions ($E_{\max} = 5.6$ eV) and the other leading to O⁻ with approximately 1 eV of translational energy ($E_{\max} = 6.1$ eV). We do not know whether the thermal and energetic O⁻ ions emanate from different exit channels on a single

surface or from two distinct surfaces. Interestingly, Lobo et al. (K + CH₃NO₂) also observed two O⁻ signals, one of which was delayed relative to the other and which they attributed to rearrangement of the CH₃NO₂⁻ (2B_1 , ground state) to CH₃ONO⁻ prior to fragmentation [28]. In the present work, the two distinct O⁻ signals certainly come from an excited

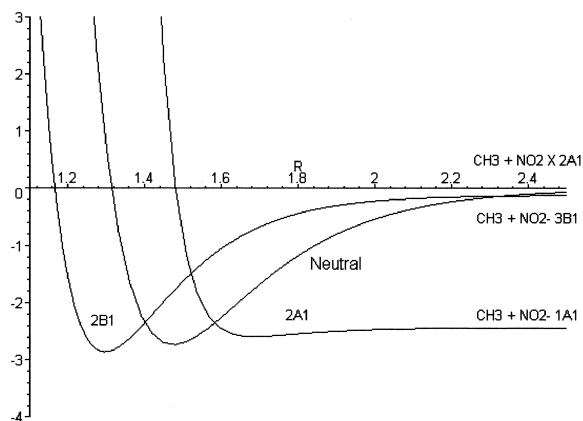


Fig. 6. Qualitative potential energy curves (energy in eV vs. internuclear distance in Å) for neutral ground-state CH₃NO₂ and the two lowest-lying anionic states, 2B_1 (π^*) which dissociates to NO₂⁻, in an excited (2B_1) state and 2A_1 (σ^*) which dissociates to NO₂⁻, in its ground state (1A_1). The R coordinate is primarily C–N extension but for the anionic states important changes in N–O and C–H geometry also occur and play a role in the dynamics.

anion (or anions); it remains to be seen whether the molecular beam scattering data may be reconciled with this.

5. Concluding remarks

The present observations on the electronic states of nitromethane and its anion are in accord with earlier spectroscopic measurements and also with information extracted from analyses of alkali atom scattering processes. The behaviour of this system following electron capture to form the two lowest-lying anionic states seems clear. These states are 2B_1 (π^*) and 2A_1 (σ^*). The former is strongly bonding along the C–N coordinate while the latter is antibonding. However, perversely, the experimental evidence is that, following initial capture of a free electron, the bound state leads to C–N bond rupture by means of a curve crossing, whereas the dissociative state leads back to the intact but vibrationally excited ground-state neutral molecule. Autodetachment is an important channel from both states. Qualitative, simplified potential energy diagrams consistent with these observations are given in Fig. 6. A quantitative picture determining the shape and lifetime of the potential surfaces and the location of their crossing seam will require both more experimental work (e.g. on inelastic electron scattering) and much more extensive computations.

It seems that despite the complexity of the dynamics and the large excess of energy the processes following electron capture by nitromethane are not statistical. This system and in particular the physics of the more highly excited channels remains a challenge to both theory and experiment.

Acknowledgements

The authors are grateful to the EPSRC for the award of beam time at the Daresbury Synchrotron Source and to the Daresbury staff, Dr. M.R.F. Siggel in particular, for help and support. It is a pleasure to be associated with tributes to Alex Stamatovic, a

scientist who is distinguished not only for his outstanding achievements but also for the generosity with which he shares his discoveries, ideas, and expertise.

References

- [1] J.W. Rabelais, *J. Chem. Phys.* 57 (1972) 960.
- [2] K. Kimura, S. Kutsumata, Y. Achiba, T. Yamazaki, S. Iwata, *Handbook of He(I) Photoelectron Spectra of Fundamental Organic Molecules*, Japan Scientific Societies, Tokyo, Halsted Press, New York, 1981.
- [3] J. Niwa, S. Tajima, T. Tsuchiya, *Int. J. Mass Spectrom. Ion Phys.* 40 (1981) 287.
- [4] J.N. Murrell, B. Vidal, M.F. Guest, *J. Chem. Soc. London Faraday Trans. 2* 71 (1975) 1577.
- [5] K.L. McEwen, *J. Chem. Phys.* 32 (1960) 1801.
- [6] L.E. Harris, *J. Chem. Phys.* 58 (1973) 5615.
- [7] W.M. Flicker, O.A. Mosher, A. Kuppermann, *J. Chem. Phys.* 72 (1980) 2788.
- [8] C. Mijoule, S. Odiod, S. Fliszar, J.M. Schnur, *J. Mol. Structure (Theochem)* 149 (1987) 311.
- [9] L.J. Butler, D. Krajnovich, Y.T. Lee, G. Ondrey, R. Bersohn, *J. Chem. Phys.* 79 (1983) 1708.
- [10] N.C. Blais, *J. Chem. Phys.* 79 (1983) 1723.
- [11] K.Q. Lao, E. Jensen, P.W. Kash, L.J. Butler, *J. Chem. Phys.* 93 (1990) 3958.
- [12] D.B. Moss, K.A. Trentelman, P.L. Houston, *J. Chem. Phys.* 96 (1992) 237.
- [13] K.G. Spears, S.P. Brugge, *Chem. Phys. Lett.* 54 (1978) 373.
- [14] P.E. Schoen, M.J. Marrone, J.M. Schnur, L.S. Goldberg, *Chem. Phys. Lett.* 90 (1981) 272.
- [15] H.S. Kwok, G.Z. He, R.K. Sparks, Y.T. Lee, *Int. J. Chem. Kinet.* 13 (1981) 1125.
- [16] J.C. Mialocq, J.C. Stephenson, *Chem. Phys.* 106 (1986) 281.
- [17] I.M. Napier, R.G.W. Norrish, *Proc. R. Soc. London, Ser. A* 299 (1967) 317.
- [18] S. Zabarnick, J.W. Fleming, A.P. Baronavski, *J. Chem. Phys.* 85 (1986) 3395.
- [19] G.D. Greenblatt, H. Zuckermann, Y. Haas, *Chem. Phys. Lett.* 134 (1986) 593.
- [20] K. Honda, H. Mikuni, M. Takahasi, H. Mikuni, M. Takahasi, *Bull. Chem. Soc. Jpn.* 45 (1972) 3534.
- [21] R.N. Compton, H.S. Carman, C. Desfrancois, H. Abdoul-Carime, J.P. Schermann, J. Hendricks, S.A. Lyapustina, K.H. Bowen, *J. Chem. Phys.* 105 (1996) 8785.
- [22] G.L. Gutsev, R.J. Bartlett, *J. Chem. Phys.* 105 (1996) 8785.
- [23] E.C.M. Chen, N. Welk, E.S. Chen, W.E. Wentworth, *J. Phys. Chem.* 103 (1999) 9072.
- [24] F. Ramondo, *Can. J. Chem.* 70 (1992) 314.
- [25] J.A. Stockdale, F.J. Davis, R.N. Compton, C.E. Klots, *J. Chem. Phys.* 60 (1974) 4279.
- [26] S.Y. Tang, E.W. Rothe, G.P. Rick, *Int. J. Mass Spectrom. Ion Phys.* 14 (1974) 79.
- [27] R.N. Compton, P.W. Reinhardt, C.D. Cooper, *J. Chem. Phys.* 68 (1978) 4360.

- [28] R.F.M. Lobo, A.M.C. Moutinho, K. Lacmann, J. Los, *J. Chem. Phys.* 95 (1991) 166.
- [29] K. Jaeger, H. Henglein, *Z. Naturforsch.* 22a (1967) 700.
- [30] A. Di Domenico, J.L. Franklin, *Int. J. Mass Spectrom. Ion Phys.* 9 (1972) 171.
- [31] C.M. Sholeen, R.R. Herm, *J. Chem. Phys.* 65 (1976) 5398.
- [32] M.A.D. Fluendy, S. Lunt, *Mol. Phys.* 49 (1983) 1007.
- [33] Y.A. Gruzdkov, Y.M. Gupta, *J. Phys. Chem. A* 102 (1998) 8325.
- [34] M.H. Palmer, I.C. Walker, M.F. Guest, M.R.F. Siggel, *Chem. Phys.* 201 (1995) 381.
- [35] G.A. Keenan, I.C. Walker, D.F. Dance, *J. Phys. B* 15 (1982) 2509.
- [36] J.L. Le Garrec, O. Sidko, J.L. Queffelec, S. Hamons, J.B.A. Mitchell, B.R. Rowe, *J. Chem. Phys.* 107 (1997) 54.
- [37] M.G. Curtis, I.C. Walker, *J. Chem. Soc. Faraday Trans.* 88 (1992) 2805.
- [38] P.J. Chantry, G.J. Schulz, *Phys. Rev.* 156 (1967) 134.
- [39] M. Fenzlaff, R. Gerhard, E. Illenberger, *J. Chem. Phys.* 88 (1988) 149.
- [40] GAUSSIAN 94, Revision C.2, M.J. Frisch, G.W. Trucks, H.B. Schlegel, P.M.W. Gill, B.G. Johnson, M.A. Robb, J.R. Cheeseman, T. Keith, G.A. Petersson, J.A. Montgomery, K. Raghavachari, M.A. Al-Laham, V.G. Zakrzewski, J.V. Ortiz, J.B. Foresman, J. Cioslowski, B.B. Stefanov, A. Nanayakkara, M. Challacombe, C.Y. Peng, P.Y. Ayala, W. Chen, M.W. Wong, J.L. Andres, J.S. Binkley, D.J. Defrees, J. Baker, J.P. Stewart, M. Head-Gordon, C. Gonzalez, J.A. Pople, Gaussian, Inc., Pittsburgh, PA, 1995.
- [41] S. Nagakura, *Mol. Phys.* 3 (1960) 152.
- [42] W.D. Taylor, T.D. Allston, M.J. Moscato, G.B. Fazekas, R. Kozlowski, G.A. Takacs, *Int. J. Chem. Kin.* 12 (1980) 231.
- [43] T. McAllister, *J. Chem. Phys.* 57 (1972) 3353.
- [44] Z-L. Cai, *J. Chem. Soc. Faraday Trans.* 889 (1993) 991.